Journal of Catalysis **209,** 341–354 (2002)
doi:10.1006/jcat.2002.3601

Kinetics, FTIR, and Controlled Atmosphere EXAFS Study of the Effect of Chlorine on Pt-Supported Catalysts during Oxidation Reactions

F. J. Gracia,* J. T. Miller,† A. J. Kropf,‡ and E. E. Wolf*,[1]

*Department of Chemical Engineering, University of Notre Dame, Notre Dame, Indiana 46556; †BP Research Center, E-1F, 150 W. Warrenville Road, Naperville, Illinois 60563; and ‡Chemical Technology Division, Argonne National Laboratory, 9700 S. Cass Avenue, Argonne, Illinois 60439

Received October 23, 2001; revised March 7, 2002; accepted March 7, 2002

The poisoning effect of Cl on the activity of Pt-supported catalysts for CO, methane, and ethane oxidation has been investigated by kinetic studies and *in situ* IR and *controlled atmosphere* EXAFS spectroscopies. Catalysts containing 1.5% Pt/Al_2O_3 were prepared by incipient wetness from H_2PtCl_6 and $Pt(NH_3)_4(NO_3)_2$ precursors. The reduced catalysts have similar dispersion (0.8) as estimated by H_2 chemisorption. The Cl-free catalyst was 10 times more active than the Cl-containing catalyst during CO and ethane oxidation. Addition of HCl to the Cl-free catalyst rendered its activity identical to the catalyst prepared from Cl-containing precursors. The presence of Cl also affects the activity of 2% Pt/SiO_2 catalysts, but to a lower extent. On the Cl-free oxidation catalyst, Pt–Pt and Pt–O bonds were detected using EXAFS, suggesting that the reduced metal particles are not fully oxidized under the reaction conditions. Additionally, chemisorption of CO by the oxidized catalyst indicates that a portion of the reduced Pt atoms is exposed to the reactants. On the Cl-containing catalyst, there are also Pt–Cl as well as Pt–Pt and Pt–O bonds. The later catalyst, however, does not chemisorb CO, indicating that there are no reduced surface Pt atoms. The effect of Cl poisoning on the oxidation activity of Pt supported on silica is similar to that on alumina. IR results show that chlorine significantly reduces the amount of CO adsorbed on metallic Pt sites. At low temperature there is little CO adsorbed on the Cl-containing Pt/silica catalyst, while at higher temperature the amount of adsorbed CO increases, likely due to reduction of the oxidized surface. The catalyst activities correlate well with the amount of reduced surface sites, and a model is proposed to explain the mechanism of chloride poisoning, which is shown to occur mainly by site blocking.

Key Words: **chlorine poisoning; Pt/alumina; Pt/silica; hydrocarbon oxidation; EXAFS; IR of adsorbed CO.**

1. INTRODUCTION

The complete combustion of methane by Pt and Pd catalysts has been studied in relation to the control of polluting emissions from natural gas vehicles (NGV) (1), as well as to the oxidation of methane in turbines for power generation (2). Supported Pt catalysts are often prepared from Cl-containing precursors such as H_2PtCl_6, and it has been reported (3–14) that Cl poisons the oxidation activity of Pt. The state of the active catalyst's surface and the effect of Cl poisoning on the activity, however, have not been elucidated.

Lieske *et al.* (15) were among the first to propose a model of the various phases that could be present in a Pt/Al_2O_3 catalyst prepared from Cl precursors as a function of pretreatment conditions. These phases, however, were not correlated with the catalyst's activity. Based on temperature-programmed reduction (TPR) of Pt catalysts oxidized at different temperatures, Hwang and Yeh (16) concluded that four types of oxide species could be formed depending on the oxidation temperature. The formation of PtO_xCl_y complexes has also been suggested when catalysts are prepared from Cl-containing precursors (17–19). Burch and Loader (20) and Yang *et al.* (21) concluded that the oxidation activity of Pt and Pd catalysts is optimal for a partially oxidized and reduced surface.

Farrauto and coworkers (3), among others, reported that the presence of Cl on the catalyst reduced the methane oxidation activity of Pd/Al_2O_3, and that removal of Cl increased the catalyst's activity. Similarly, Marceau *et al.* (4, 5) found that elimination of Cl from Pt/Al_2O_3 catalysts at 450°C led to higher activity. Roth *et al.* (6) also confirmed that removal of Cl from a Pd/Al_2O_3 catalyst led to the same activity as Cl-free Pd catalysts and suggested that the active sites are PdO that slowly deactivates to form a less active $Pd(OH)_2$.

The objective of this work is to conduct a comprehensive study of the state of the surface on Cl-free and Cl-containing Pt-supported catalysts during oxidation reactions and to correlate the activity with the structure of the active Pt species under oxidizing reaction conditions. EXAFS spectroscopy is used to probe the local structure around the Pt atom, and *in situ* IR spectroscopy is used to analyze the state of the catalytic surface and adsorbed species under reaction conditions.

[1] To whom correspondence should be addressed. Fax: (1-219) 631-8366. E-mail: Eduardo.E.Wolf.1@nd.edu.

0021-9517/02 $35.00

2. EXPERIMENTAL

2.1. Catalyst Preparation

To investigate the effect of chlorine on the activity of Pt-supported catalysts, samples were prepared from H_2PtCl_6 (*with Cl*) and $Pt(NH_3)_4(NO_3)_2$ (*no Cl*) on alumina and silica supports.

1.5% Pt/Alumina (with Cl). To 11.7 g of Catapal alumina calcined at 500°C (SA = 203 m^2/g, pore volume = 0.42 cc/g) was added 0.467 g of H_2PtCl_6 (37.5% Pt) in 9 ml of H_2O. The catalyst was dried and calcined at 500°C for 2 h. Elemental analysis indicated 2.1% Cl, and the hydrogen chemisorption ($T = 25$°C) of the reduced catalyst was 0.71 cm^3/g, or a dispersion of 0.82.

1.5% Pt/Alumina (no Cl). To 15.0 g of Catapal alumina was added 0.60 g of $Pt(NH_3)_4(NO_3)_2$ in 11 ml of H_2O. The catalyst was dried overnight and calcined at 250°C for 2 h. The hydrogen chemisorption of the reduced catalyst (T = 25°C) was 0.70 cm^3/g, or a dispersion of 0.81.

2.0% Pt/SiO_2 (no Cl). To 40.0 g of Davison grade 644 silica (SA = 284 m^2/g, pore volume = 1.12 c^3/g) was added 1.6 g of $Pt(NH_3)_4(NO_3)_2$ in 65 ml of H_2O. The catalyst was dried overnight and calcined at 225°C for 3 h. This catalyst showed a dispersion of 0.36 as measured by hydrogen chemisorption.

After calcinations, the catalysts were reduced in flowing H_2 (200 cc/min) at 300°C for 2 h. The prereduced catalysts were pretreated in air prior to activity, IR, EXAFS, and CO chemisorption measurements.

Fractions of the Cl-free catalysts were treated with HCl using wet impregnation followed by overnight drying at 110°C to analyze the effect of Cl addition to the Cl-free catalyst from sources different than the precursor.

2.2. Catalytic Activity

Catalyst activities were determined in a tubular-flow microreactor with recycle at atmospheric pressure. The catalyst (100 mg) was placed in a quartz tube (12 in. long, 0.5-in. diameter) equipped with an external recycle pump. A thermocouple was set in the center of the catalyst bed to monitor the temperature of the bed. The effluent flow rate was 130 cm^3/min, and the recycle ratio was about 20 to ensure complete mixing. Only small differences in activity were obtained for (prereduced) catalysts pretreated in air or in H_2 followed by calcination in air. Hence, prior to each run, the catalysts were pretreated in air at 300°C for 2 h. The catalysts were then cooled to room temperature and switched to the reaction mixture, and the temperature was increased to about 450°C. (Hydrogen chemisorption of metallic Pt particles oxidized up to 500°C showed no significant change in dispersion.) Catalyst activities were measured under diluted reactant concentrations: 0.3% CO, CH_4, or C_2H_6 and an oxidizing atmosphere with 16% O_2, balanced in He. The product gases were analyzed by gas chromatography (Varian 920) equipped with a thermal conductivity (TC) detector using a Hayasep Q column at room temperature. The conversion data were reproducible within 5% accuracy. Reaction rates were calculated at various temperatures directly from the conversion assuming complete mixing due to the large recycle ratio used. Turnover frequencies were calculated from rate, and dispersion values were obtained for the freshly reduced catalysts and plotted vs $1/T$ to obtain activation energies.

2.3. EXAFS Experiment

Measurements using extended X-ray absorption fine-structure (EXAFS) spectroscopy were made on the insertion-device beamline of the Materials Research Collaborative Access Team (MR-CAT) at the Advanced Photon Source, Argonne National Laboratory. Measurements were made in the transmission mode with ionization chambers optimized for the maximum current with linear response (~10^{10} photons detected/s). A cryogenically cooled double-crystal Si(111) monochromator with resolution (ΔE) better than 2.5 eV at 11.564 keV (Pt L_3 edge) was used in conjunction with a Rh-coated mirror to minimize the presence of harmonics (22).

The samples were pressed into a cylindrical holder with a thickness chosen to give an absorbance ($\Delta \mu x$) of about 1.0 in the Pt edge region, corresponding to approximately 100 mg of catalyst. The sample holder was centered in a continuous-flow EXAFS reactor tube (18 in. long, 0.75-in. diameter) fitted at both ends with polyimide windows and valves to isolate the reactor from the atmosphere after a pretreatment had been conducted. The catalysts were pretreated outside the EXAFS data acquisition room by flowing gases or reactants at temperatures similar to those used for pretreatment or reaction during the catalytic activity measurements. After the prescribed treatment, the sample was cooled to room temperature and, then, the cell was isolated and moved to the EXAFS instrument room, with the catalysts kept exposed to the same reactant mixture in which the pretreatment was made. This prevented changes in the chemical state of the catalytic surface after the pretreatments and during the EXAFS runs, so the experiments were equivalent to being under *in situ* conditions since the catalysts were never taken off the reactor tube. Thus, the state of the surface probed during EXAFS should be the same as after pre-treatment.

The EXAFS of *calcined* (300°C, air) catalysts were first measured in air at room temperature. These catalysts were then reduced in 5% H_2 (balance He) at 300°C for 1 h and cooled to room temperature, and EXAFS data were collected in H_2 (*reduced*). Thereafter, the prereduced catalysts

were purged with He at room temperature, then heated to 300°C in 5% O_2 (balance He) for 1 h (*oxidized*). After the oxidizing pretreatment, the EXAFS data were collected at room temperature in O_2.

2.4. FTIR Spectroscopy

Transmission infrared spectra of pressed disks (14 mg) of Pt/SiO_2 with and without Cl were collected in a FTIR spectrometer (Mattson, Galaxy 6020) at a resolution of 2 cm^{-1} and 30 scans/spectrum. The self-supporting disks were placed in an IR cell equipped with NaCl windows and a temperature controller. The samples were pretreated in air at 200°C for 1 h prior to measurement of CO adsorption, oxidation, and desorption. After calcination, the catalyst was cooled to room temperature in He and 0.3% CO was added to the feed to measure CO adsorption. During the CO oxidation experiments, 16% O_2 was added to the CO-containing feed. In both experiments, the heating rate was 1°C/min with a total flow of 120 cm^3/min. Before CO desorption studies, the cell containing the pretreated catalyst was purged with pure He at 200°C for 1 h and 0.3% CO in He was then added. The saturation level for CO adsorption was rapidly reached. The spectra were collected as a function of time at 200°C under a flow of pure He. The spectra were obtained in the absorbance mode after subtraction of the background spectrum of each catalyst disk under He atmosphere at the corresponding temperature.

3. RESULTS

3.1. Catalytic Activity

The effect of Cl on CO, methane, and ethane oxidation reactions on Pt/Al_2O_3 catalysts is shown in Fig. 1. The plots in the left panels correspond to the conversion at different temperatures and those in the right to the Arrhenius plots. The TOF values used in the Arrhenius plots were obtained at low conversion (<15%) to minimize the effect of reactant concentration.

During CO oxidation (Fig. 1A), even though both catalysts have nearly identical Pt loading and particle size, the catalyst prepared from H_2PtCl_6 (2.0 wt% Cl) requires about 50°C higher temperature to obtain the same CO conversion. This corresponds to a 10-fold change in reaction rate (units of moles of CO_2 produced per second per mole of surface Pt) at 100°C. From the Arrhenius plots, activation energies of 87.1 and 59.9 kJ/mol for the Cl-containing and Cl-free catalyst, respectively, were obtained. The broken line reflects TOF values recalculated using IR corrections. These results are discussed later, in Section 4.

For CH_4 oxidation, the lighting off temperature (LOT, temperature at which 50% conversion is reached) is much higher than for CO oxidation. In this case, the Cl-free catalyst is also more active than the Cl-containing catalyst. As shown in Fig. 1B, the presence of chlorine results in an increase of 100°C in the temperature at which a CH_4 conversion of 50% is reached. At 350°C, the reaction rate of the Cl-containing catalyst is 20 times slower than that of the catalyst with no Cl. In this case, the corresponding activation energies are 107.5 kJ/mol (with Cl) and 90.9 kJ/mol (no Cl).

For the complete oxidation of ethane (Fig. 1C), when chlorine is present, there is an 80°C shift of the conversion curve compared to that of the Cl-free catalyst. This corresponds to a 10-fold difference in the reaction rate at 330°C. Calculations from the Arrhenius plots yield similar activation energies of 68.6 kJ/mol (with Cl) and 68.2 kJ/mol (no Cl). The results presented in Fig. 1 clearly show that Cl decreases the activity of Pt/alumina catalysts during CO, CH_4, and C_2H_6 oxidation reactions.

To further demonstrate the effect of Cl on the oxidation activity, HCl was added at room temperature to the Cl-free catalyst to give a Cl content of about 2 wt%, which is similar to the Cl present on the catalyst prepared from chloroplatinic acid. After impregnation with HCl, the catalyst was dried overnight at 110°C and subjected to different pretreatments in air prior to reaction. Figure 2 shows the CO conversion curves as a function of the pretreatment temperature for these catalysts. When the impregnated catalyst underwent reaction without any calcination treatment, there was only a minor decrease in the activity compared to the Cl-free catalyst (Fig. 2A). This suggested that Cl was adsorbed mainly on the alumina support without affecting the Pt surface. When the same catalyst was calcined at 250°C, the activity decreased significantly (Fig. 2B), indicating that during the calcination pretreatment, Cl migrated from the support and readsorbed on the Pt surface, poisoning its activity. A further increase in the calcination temperature of a freshly impregnated catalyst gave a catalytic activity closer to that of the Cl-containing catalyst (Fig. 2C).

The amount of Cl (added as HCl) is also a factor in decreasing the CO oxidation activity of the Cl-free catalyst, as shown in Fig. 3. After impregnation with an HCl solution containing about 5 wt% followed by calcination, the activity of the catalyst with no Cl decreased below that of the catalyst prepared from a Cl-containing precursor. Calcination in air at 300°C (Fig. 3B) lowers the LOT compared to the same catalyst pretreated at 250°C (Fig. 3A), i.e., increases the activity. This indicates that when present beyond a certain saturation value, the excess chlorine is removed from the Pt particles by pretreatment in air at 300°C. For methane oxidation, however, the calcination treatment after HCl addition had little effect on the catalyst activity (Fig. 4). In this case, the reaction starts at a temperature higher than the calcination temperature of 300°C (Figs. 4C and 4D); therefore, heating the catalyst to the reaction temperature is equivalent to pretreating it in air. Addition of excess Cl (5 wt% Cl) had no additional effect on the methane oxidation activity

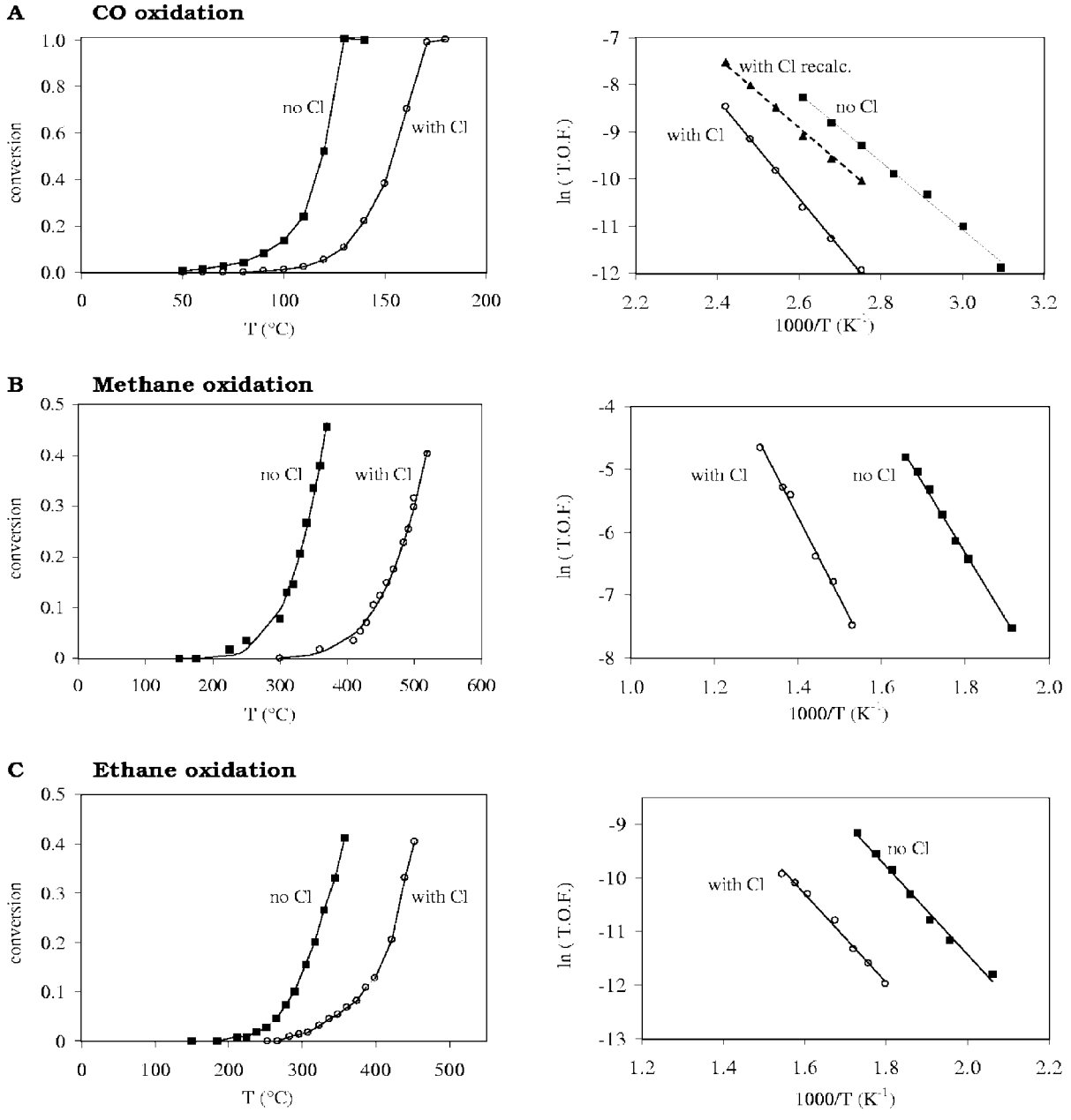

FIG. 1. Oxidation reactions on Pt/alumina catalysts with and without Cl. (Left panel) Conversion vs temperature; (right panel) Arrhenius plots. (A) CO oxidation. Broken line indicates TOF recalculated using IR corrections. (B) CH_4 oxidation. (C) C_2H_6 oxidation. Feed composition: 0.3% CO, CH_4, or C_2H_6; 16% O_2; balance He. Total flow rate, 130 cm^3/min. Recycle reactor.

(Fig. 4E), also indicating a saturation of the Cl coverage of the Pt surface.

The poisoning effect of chlorine shown for Pt supported on alumina catalysts also occurs in the case of Pt supported on silica (Fig. 5). After addition of Cl by impregnation with HCl, the LOT for CO oxidation on the Pt/silica catalyst is 45°C higher than with the Cl-free catalyst. At 120°C the reaction rate of the Cl-containing catalyst is 30 times lower than that of the Cl-free one. A direct quantitative comparison of the effect of chlorine on silica and alumina cannot be made because of the different dispersion of Pt on each support. After prolonged treatments of the catalysts the effect of Cl is different on the silica support than on alumina. As shown in Fig. 5, after reduction in H_2 at 300°C for 10 h, the activity of the Cl-containing Pt/silica catalyst increases and recovers to a level similar to that of the Cl-free catalyst. This indicates that on the silica support most of the Cl has been removed by the reduction treatment. In contrast, after treatment in H_2 for 40 h at 450°C, the activity for CO oxidation on the Cl-containing Pt/Al_2O_3 catalyst

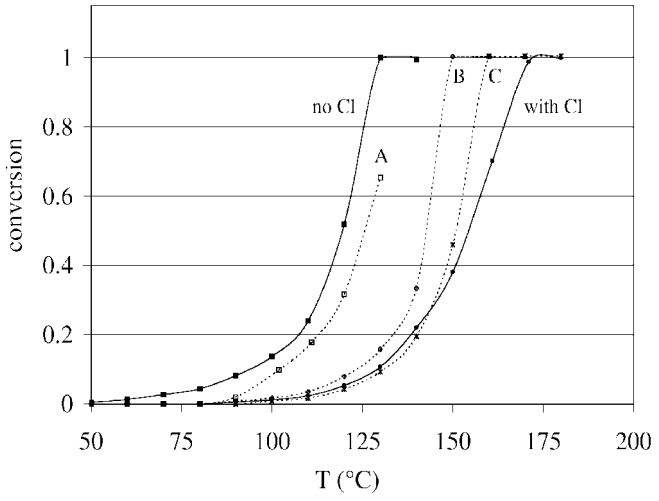

FIG. 2. Effect of calcination temperature after impregnation with HCl during CO oxidation of Pt/alumina catalyst. (A) No calcination treatment. (B) Calcination at 250°C. (C) Calcination at 300°C. Feed composition: 0.3% CO, 16% O_2, balance He. Total flow rate, 130 cm^3/min. Recycle reactor.

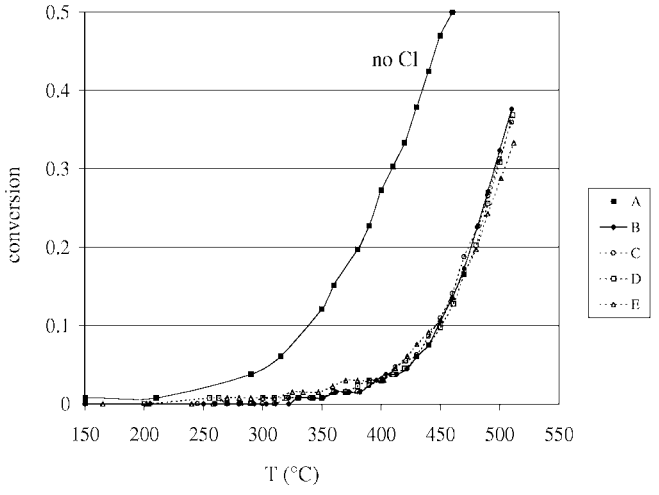

FIG. 4. Methane conversion vs temperature for Pt/alumina catalysts prepared by different methods. (A) Cl-free catalyst. (B) Cl-containing catalyst prepared from H_2PtCl_6. (C) Cl-free catalyst impregnated with 2% HCl solution, calcined at 250°C. (D) Cl-free catalyst impregnated with 2% HCl solution, calcined at 300°C. (E) Cl-free catalyst impregnated with 5% HCl solution, calcined at 300°C. Feed composition: 0.3% CH_4, 16% O_2, balance He. Total flow rate, 130 cm^3/min. Recycle reactor.

showed no improvement. These results indicate that Cl is more strongly adsorbed on the surface of the alumina support than on silica.

Figure 6 shows the effect of other pretreatments on the activity of Pt/alumina catalysts. Both catalysts, Cl-free (Fig. 6A) and with Cl (Fig. 6B), were subjected to reduction/oxidation pretreatments before CO oxidation. After the initial impregnation with the corresponding Pt-containing salt and overnight drying, fractions of each sample were either calcined in air (calcined) or reduced in H_2 (reduced) at 300°C for 2 h. For the Cl-free catalyst, the activity of the calcined sample was approximately 10 times lower than that of the reduced one, and approximately the same as the Cl-containing catalyst in Fig. 1A. Oxidation of the reduced Cl-free catalysts at 300°C in air did not much alter its activity. For the Cl-containing catalyst again the reduced sample is significantly more active than the calcined catalyst (Fig. 6B). The activity of the reduced Pt/alumina (with Cl), however, remains five times lower than that of the Cl-free catalyst. Oxidation of the reduced catalyst in air resulted

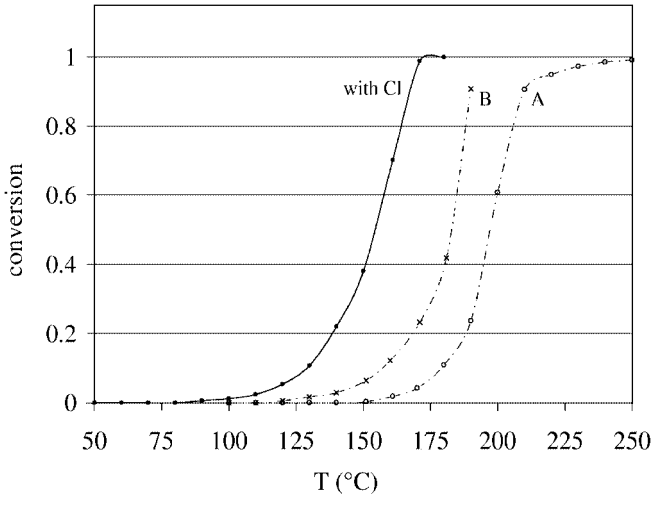

FIG. 3. Effect of calcinations temperature after impregnation in excess with HCl during CO oxidation of Pt/alumina catalyst. (A) Calcination at 250°C. (B) Calcination at 300°C. Feed composition: 0.3% CO, 16% O_2, balance He. Total flow rate, 130 cm^3/min. Recycle reactor.

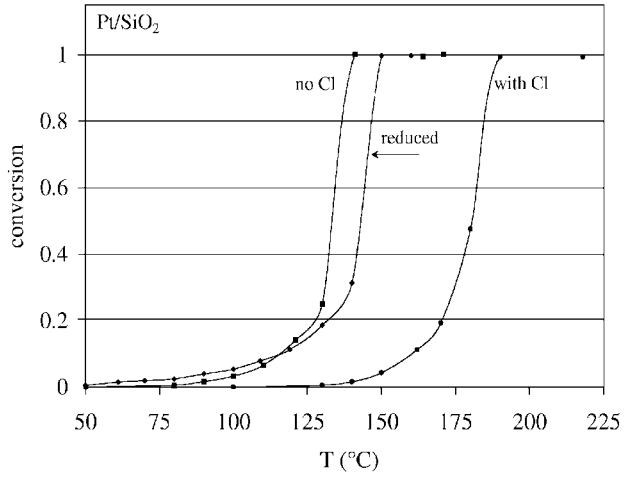

FIG. 5. CO conversion vs temperature for Pt/silica catalysts. (No Cl) 1.5% Pt/silica no Cl. (With Cl) 1.5% Pt/silica with Cl. (Reduced) 1.5% Pt/silica with Cl after reduction treatment for 10 h at 300°C. Feed composition: 0.3% CO, 16% O_2, balance He. Total flow rate, 130 cm^3/min. Recycle reactor.

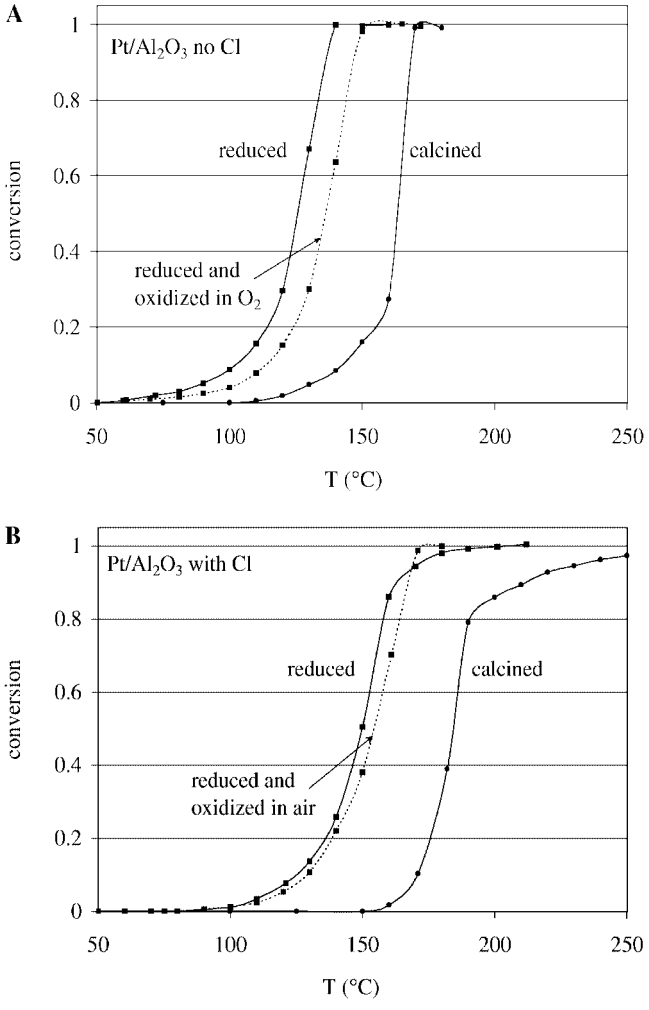

FIG. 6. Effect of pretreatment on the activity of Pt/alumina catalysts during CO oxidation. (A) 1.5% Pt/alumina no Cl. (B) 1.5% Pt/alumina with Cl. Feed composition: 0.3% CO, 16% O_2, balance He. Total flow rate, 130 cm^3/min. Recycle reactor.

in slightly lower activity. This indicates that the reduced Pt particles are relatively stable (20, 23) and a good proportion of them remain in the reduced state after 300°C oxidation treatment. This is later confirmed, in Sections 3.2 and 3.3, by data from EXAFS and FTIR analyses, respectively. Figure 6A shows that even after using more oxidizing conditions, such as pure oxygen (instead of air) at 350°C for 2 h, the activity of the Cl-free catalyst decreased but is still considerably higher than that of the calcined catalyst, suggesting that the oxidation only occurred in a fraction of the active metal.

3.2. EXAFS Analysis

Standard procedures based on WINXAS97 software (24) were used to extract the EXAFS data (25). Phase shifts and backscattering amplitudes were obtained from EXAFS data for reference compounds: $Na_2Pt(OH)_6$ for Pt–O, H_2PtCl_6 for Pt–Cl, and Pt foil for Pt–Pt.

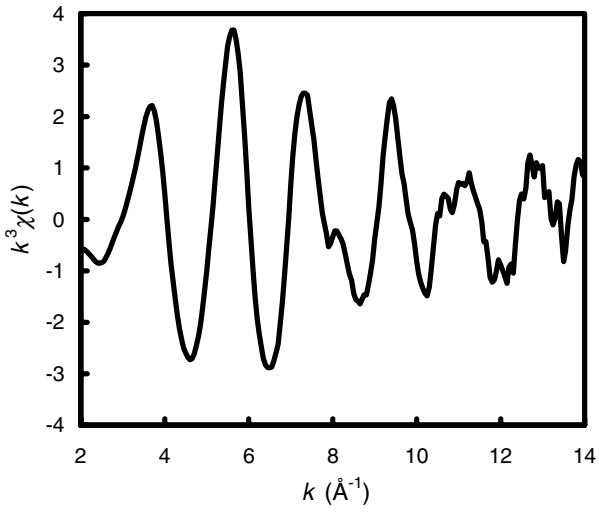

FIG. 7. Raw EXAFS data for 1.5% Pt/Alumina (no Cl).

The EXAFS data were collected for the *calcined*, *reduced*, and *oxidized* Pt catalysts. A typical spectrum of the raw data for the oxidized catalyst without Cl is shown in Fig. 7. Multiple-shell-model fits of the forward and inverse k^3 weighted (or k^2 for Pt–O only) EXAFS data were obtained between k = 3.1–12.5 $Å^{-1}$ and r = 1.3–3.0 Å, respectively. The fitting parameters are summarized in Table 1.

The EXAFS results of the *calcined* Cl-free catalysts fits a model having Pt with six oxygen nearest neighbors with the Pt–O distance of about 2.06 Å. No Pt–Pt bonds were observed in the calcined catalysts. The XANES spectra for

TABLE 1

Results from EXAFS Fitting

Treatment	Scattering path	Coord. no.	R (Å)	$\Delta\sigma^2$ ($Å^2$) ($\times 10^3$)	ΔE_o (eV)
1.5% Pt/alumina (no Cl)					
Calcined at 250°C	Pt–O	5.9	2.06	0.5	1.8
Reduced at 300°C	Pt–O	1.1	2.19	10.6	17.5
	Pt–Pt	6.6	2.74	2.4	−3.0
Oxidized at 300°C, 5% O_2	Pt–O	3.9	2.04	4.5	0.8
	Pt–Pt	3.6	2.70	8.3	−0.9
1.5% Pt/alumina (with Cl)					
Calcined at 300°C	Pt–O	3.5	2.03	−1.4	−0.2
	Pt–Cl	2.5	2.31	−1.4	−1.2
Reduced at 300°C	Pt–O	0.9	2.21	2.2	17.4
	Pt–Pt	6.9	2.74	2.4	−2.9
Oxidized at 300°C, 5% O_2	Pt–O	2.0	2.05	4.6	1.6
	Pt–Cl	2.5	2.31	4.6	5.2
	Pt–Pt	0.9	2.70	1.5	−0.5

Note. k^3, Δk = 3.1–12.5, Δr = 1.3–3.0.

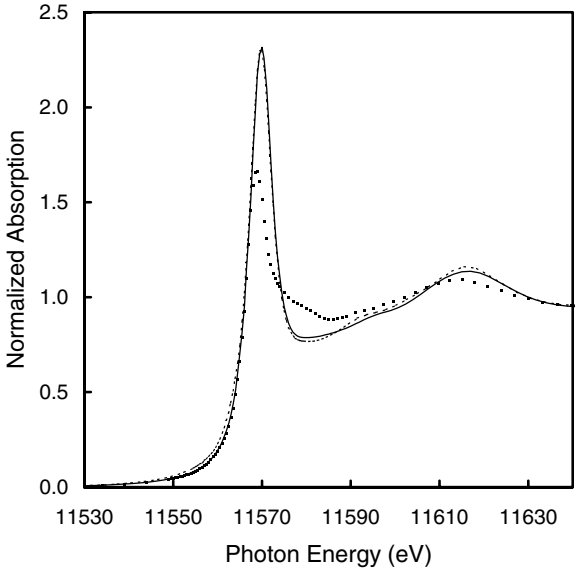

FIG. 8. XANES spectra for 1.5% Pt/Alumina (no Cl) calcined at 250°C (solid line), for $Pt(NH_3)_4(NO_3)_2$ (dotted line), and for $Na_2Pt(OH)_6$ (dashed line).

the calcined catalyst, $Pt(NH_3)_4(NO_3)_2$, and $Na_2Pt(OH)_6$ are shown in Fig. 8. Both the position and intensity of the XANES spectrum of the calcined catalyst are consistent with Pt in the +4 oxidation state. After reduction at 300°C, small metallic Pt particles are formed, as evidenced by the 6.6 Pt–Pt coordination number and a bond distance of 2.74 Å. A fully coordinated shell in Pt metal consists of 12 nearest-neighbor Pt atoms at a distance of 2.77 Å. The EXAFS of the reduced catalyst also show a contribution from the oxygen ions of the support with a Pt–O distance at about 2.19 Å, which is similar to that previously reported by Vaarkamp *et al.* (26) for fully reduced Pt, Rh, and Ir catalysts. In the EXAFS of the oxidized catalyst, the Pt–Pt coordination number decreases to 3.6 at a distance of 2.70 Å. In addition, there is a significant Pt–O contribution at a distance of 2.04 Å with a coordination number of 3.9. The XANES spectra of the calcined, reduced (with chemisorbed H_2), and oxidized Pt/alumina (no Cl) catalysts and Pt foil are shown in Fig. 9. The onset of the edge in the oxidized catalyst is similar to that in the reduced catalyst; however, the intensity of the white line is significantly higher. The XANES spectrum is consistent with the presence of reduced and oxidized Pt atoms.

The EXAFS and XANES spectra (not shown) of the *calcined* Pt/Al_2O_3 (with Cl) catalyst fits a model where the Pt(IV) is bonded to 3.5 oxygen ions at a distance of 2.05 Å and to 2.5 chloride ions at a distance of 2.31 Å. The Pt–Cl distance is identical (within experimental error) to that in chloroplatinic acid (27). After reduction at 300°C, small metallic Pt particles are again formed with a Pt–Pt coordination number of 6.9 at a distance of 2.74 Å. There is also the small Pt–O coordination of 0.9 from the oxygen ions of the support at a distance of 2.21 Å (26). The EXAFS of the reduced Cl-containing catalyst is very similar to that of the Cl-free catalyst. It should be noted that there are no Pt–Cl bonds in the reduced catalyst, even though this catalyst originally contained 2 wt% Cl. The coordination numbers of 6.6 and 6.9 Pt neighbors for the two reduced catalysts in Table 1 show that, on average, the first shell of every Pt atom is not completely coordinated to Pt, indicating small metallic Pt particles. Assuming a compact geometry and that the Debye–Waller factor, σ^2, has been modeled correctly, the average particle diameter is 9 ± 3 Å. These values are consistent with the H_2 chemisorption results, indicating that the dispersions are 0.8.

The EXAFS results of the Cl-containing catalyst oxidized at 300°C fit a model with a Pt–Pt distance of 2.70 Å and a coordination number of 0.9, indicating the presence of small metallic Pt particles that are not fully oxidized. Although the size of the reduced Pt particles in both catalysts is very similar, upon oxidation, the catalyst that contains Cl is more fully oxidized, leading to a smaller Pt–Pt coordination number. These results are consistent with those reported by Borgna *et al.* (40), which indicate that during oxidation of a nonchlorinated Pt/Al_2O_3 catalyst, only a single coating of PtO_2 is formed, whereas the presence of Cl is responsible for a deeper attack of Pt particles, causing the formation of a double coating of oxychloroplatinum species. In addition, the Pt–O and Pt–Cl coordination numbers are 2.0 and 2.5 at a distance of 2.05 and 2.31 Å, respectively. Figure 10 shows the k^3-weighted Fourier transform of the EXAFS and the

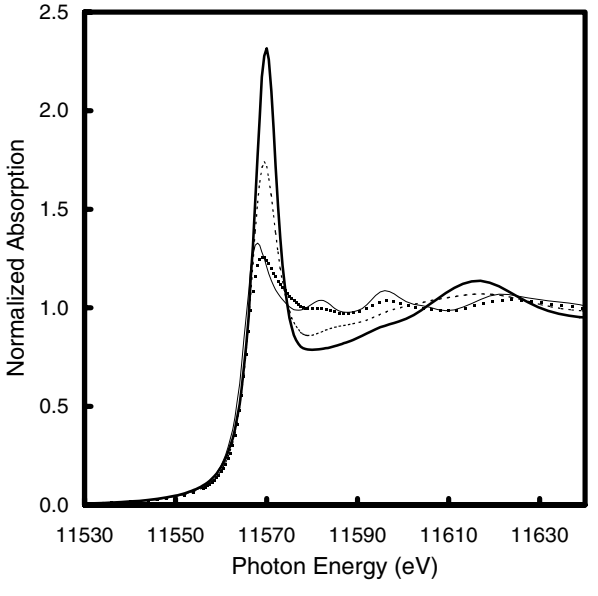

FIG. 9. XANES spectra of 1.5% Pt/Alumina (no Cl) calcined at 250°C (solid line), reduced at 300°C and with chemisorbed H_2 (dotted line), and oxidized at 300°C (dashed line) and for Pt foil (fine solid line).

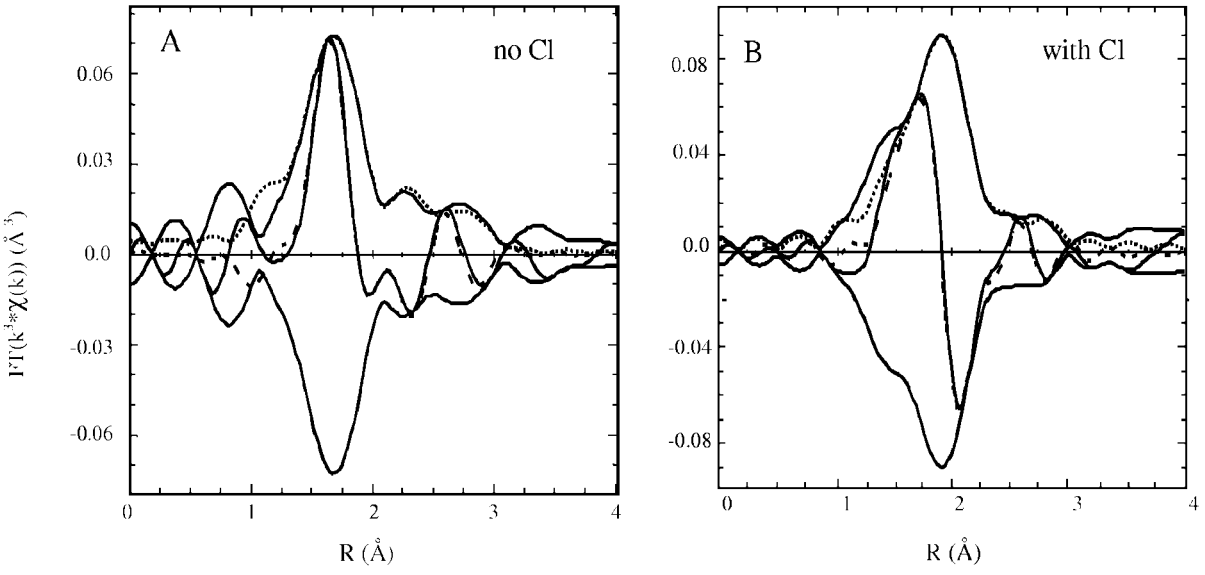

FIG. 10. k^3-weighted Fourier transform (magnitude and imaginary part) of Pt EXAFS. (solid lines) Raw data; (dotted lines) model fit. (A) 1.5% Pt/alumina no Cl. (B) 1.5% Pt/alumina with Cl.

model fit for the oxidized Cl-free and Cl-containing Pt catalysts. Even though the magnitudes of the transforms are similar, the imaginary components are significantly different, an effect of the addition of 2.5 Cl neighbors, as shown in Fig. 10B. Thus, although there are no Pt–Cl bonds in the reduced catalyst, upon heating in O_2 to 300°C, Pt–Cl bonds are clearly present after oxidation of the catalyst. This confirms that, as suggested by the activity results, Cl present on the support migrates to the metal surface during oxidation. Similar results were obtained for both oxidized catalysts treated with 4% O_2 alone, 0.3% CH_4, and 16% O_2, or 3% CH_4 and 16% O_2 at 300 and 450°C, showing that slightly different reaction environments lead to similar surface states.

For both Pt/alumina catalysts, subsequent reduction at 300°C following oxidation or reaction up to 450°C gives identical EXAFS spectra and fit results to those of the initially reduced catalysts, indicating that there is no sintering during catalytic oxidation below 450°C.

3.3. CO Chemisorption and FTIR of Adsorbed CO

The amount of CO chemisorbed at room temperature was determined for several calcined and oxidized Pt/alumina catalysts. On both calcined catalysts (with and without Cl), within experimental error there was little chemisorption of CO. Also, on the (reduced) Pt/alumina (with Cl) oxidized at 300°C, there was little chemisorbed CO. However, oxidation in air of the reduced Pt/alumina (no Cl) gave significant adsorption, 0.70 cm^3/g, or about 40% of the Pt atoms chemisorb CO. The chemisorption results suggest that many of the metallic or low-valent Pt atoms of the Pt/alumina (no Cl) are exposed to the reacting gases. In addition, since the metallic Pt in the oxidized Pt/alumina (with Cl) does not chemisorb CO, these atoms are not at the particle surface and thus are likely covered by oxygen and Cl atoms.

The infrared spectra on Pt/silica oxidation catalysts were obtained in order to further investigate the effect that Cl has on the adsorption, desorption, and reaction of CO on Pt-supported catalysts. SiO_2 was chosen as the support because of its higher transmissivity compared to Al_2O_3. Figure 11 shows the spectra for CO adsorption on Cl-free Pt/SiO_2 (Fig. 11A) and with Cl (Fig. 11B) in the range 2300–1800 cm^{-1}. The spectra are consistent with the presence of linearly adsorbed CO on Pt (11, 18, 28–31), indicating that at low CO concentration (0.3% CO in He) the catalyst with no Cl rapidly adsorbs CO at the various temperatures analyzed. In addition, two weak IR bands were detected in the region 2200–2100 cm^{-1}, corresponding to CO in the gas phase. The spectra in Fig. 11 show that the peak at 2079 cm^{-1} shifts to lower wavenumbers as the temperature increases (2065 cm^{-1} at 200°C). Hertz and Shinouskis observed a frequency shift (from 2120 to 2070 cm^{-1}) of the linearly adsorbed CO peak during transient reduction experiments on Pt-supported catalysts (32). They correlate this shift with a change in the electronic state of Pt atoms. The higher frequency is assigned to completely oxidized Pt particles (Pt^{m+} with $2 \geq m > 1$) and the subsequent lower frequencies to CO adsorbed on Pt atoms presenting lower oxidation states (Pt^{n+} at 2095 cm^{-1} and $Pt^{\delta+}$ at 2080 cm^{-1} with $1 \geq n > \delta$). Finally, a band at 2070 cm^{-1} is characteristic of linear CO adsorption on fully reduced Pt. Since the integrated absorbance of this peak remains almost constant and considering that the catalyst was previously calcined in air, the observed shift is attributed to a gradual reduction

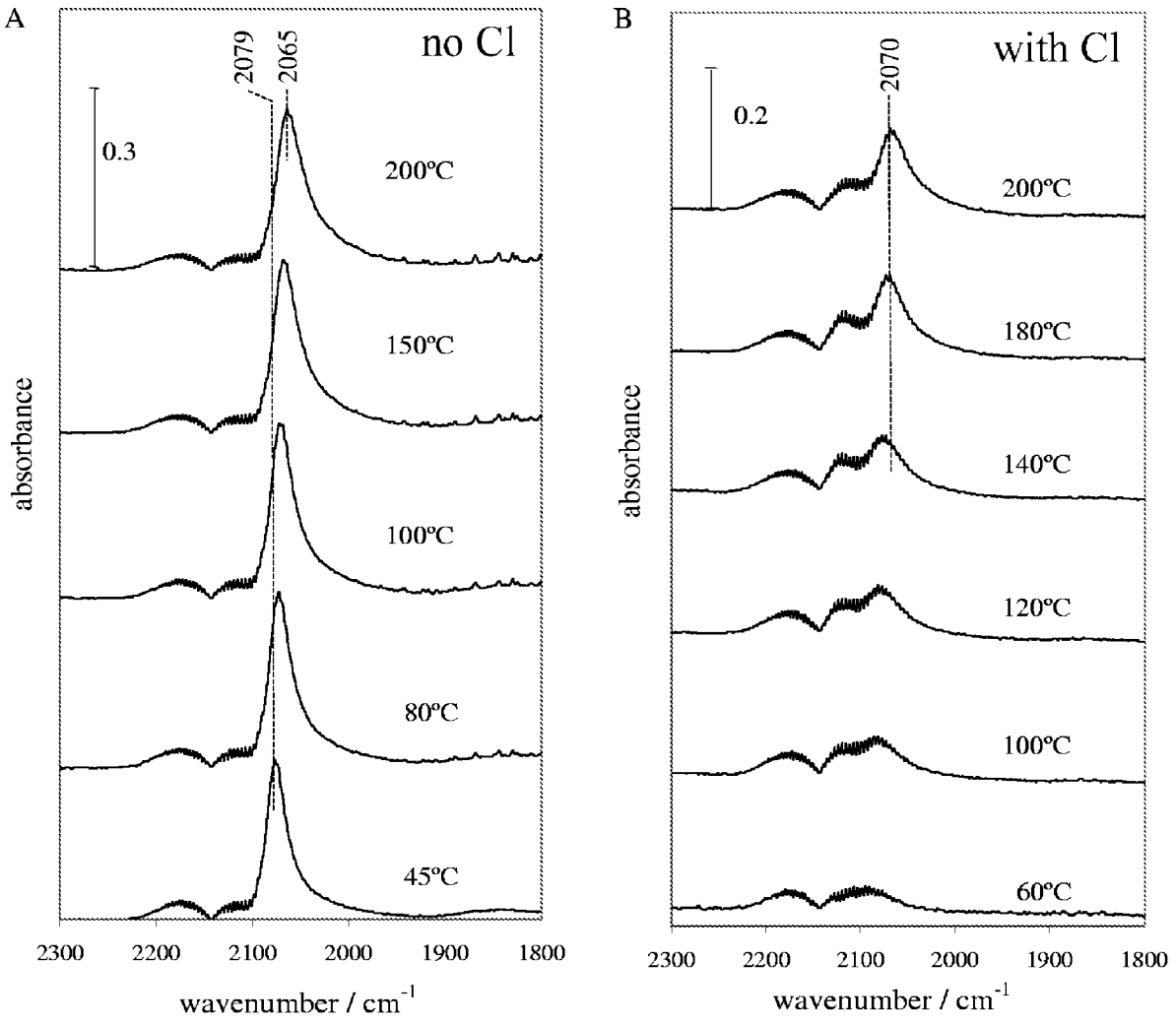

FIG. 11. FTIR spectra during CO adsorption on Pt/silica. (A) 2% Pt/silica no Cl. (B) 2% Pt/silica with Cl. Feed composition: 0.3% CO, balance He. Total flow rate, 120 cm^3/min.

of partially oxidized $Pt^{\delta+}$ atoms at the higher temperatures due to the presence of CO.

When Cl is present on the surface, the signal of adsorbed CO is almost below the detection level at the lower temperatures ($T < 100$°C, Fig. 11B). As the surface temperature increases, the amount of adsorbed CO increases slightly, but it does not reach a level comparable to that observed in the Cl-free sample. These results indicate that Cl is blocking the sites for CO adsorption.

To verify this conclusion, both catalysts were subjected to the same reaction gas compositions used in the activity determinations (0.3% CO, 16% O_2, in He) and the corresponding IR spectra were collected at different temperatures (Fig. 12). On the Pt/SiO_2 (no Cl) catalyst, a peak at a constant wavenumber of 2077 cm^{-1} is observed at temperatures as low as 65°C. The intensity of this peak remains constant with temperature, indicating saturation of the active sites with adsorbed CO until ignition of the catalyst is reached, between 140 and 145°C. At temperatures above 145°C, the surface coverage of adsorbed CO is below the detection limit, indicating complete and immediate reaction. After ignition, a peak at 2321 cm^{-1} appears, corresponding to CO_2 in the gas phase. During this TPR experiment, no shift in the position of the peak at 2077 cm^{-1} is observed, indicating that in this oxidizing atmosphere the Pt oxidation state remains unchanged. Comparison between the activity results and the IR spectra of CO oxidation on Pt/SiO_2 catalysts shows remarkable agreement regarding the temperatures at which each state of the reaction occurs (low-activity regime, ignition, and high-activity regime), allowing one to correlate the kinetic behavior reported in Section 3.1 with the state of the surface inferred from IR spectroscopy.

At temperatures below 140°C, addition of chlorine leads to a significant decrease in the amount of adsorbed CO (Fig. 12B). As the temperature increases from 60 to about 185°C, before reaction, there is a slow increase in the

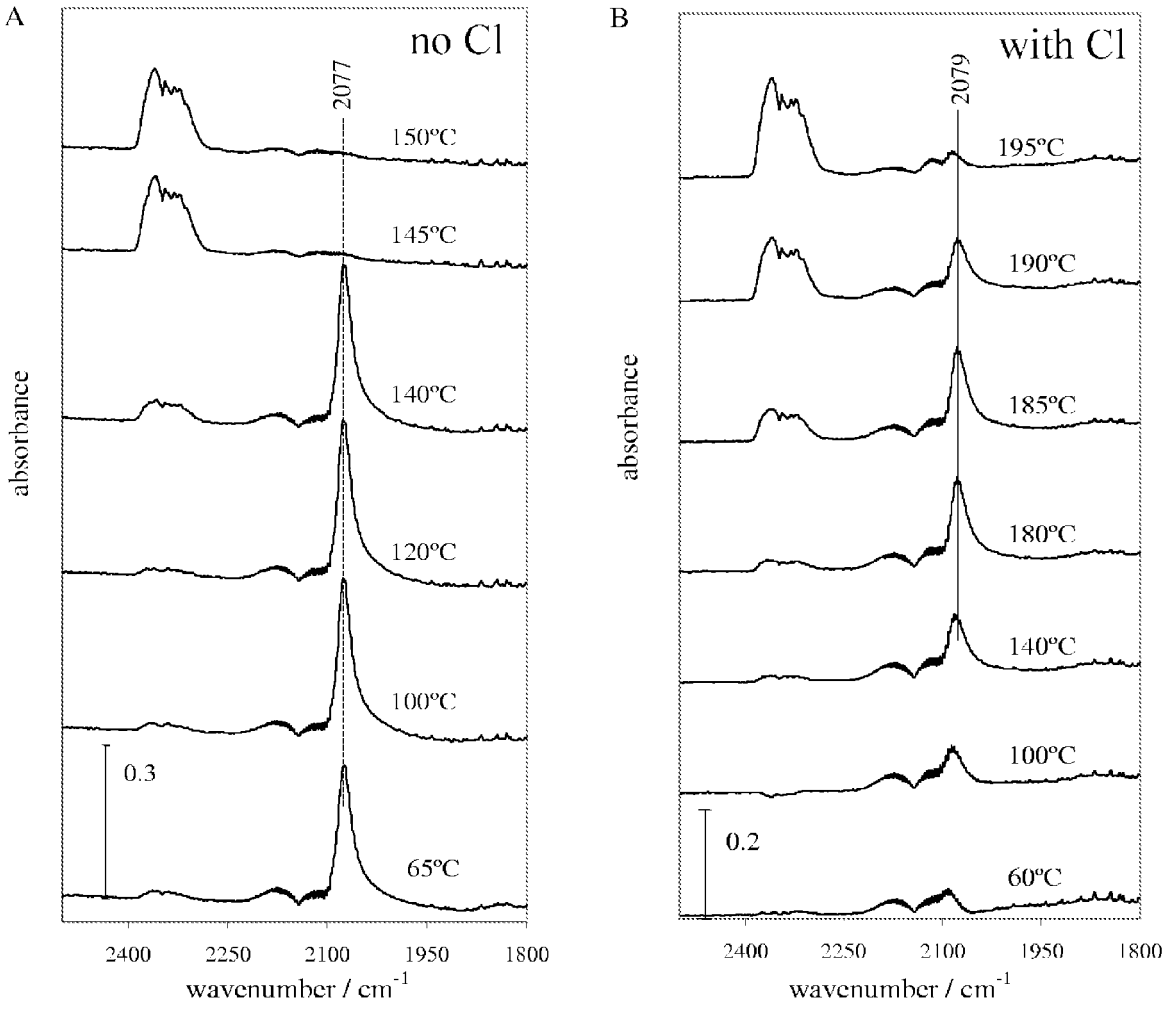

FIG. 12. FTIR spectra during CO oxidation on Pt/silica. (A) 2% Pt/silica no Cl. (B) 2% Pt/silica with Cl. Feed composition: 0.3% CO, 16% O_2, balance He. Total flow rate, 120 cm^3/min.

amount of CO adsorbed. Above 185°C, the CO surface coverage decreases until 190°C, where there is little adsorbed CO due to consumption by the reaction. Chlorine not only decreases the number of sites available for reaction, it also slows down the ignition process. This is seen by the larger temperature difference (15°C) required for ignition with the Cl-containing catalyst compared with that (5°C) when no chlorine is present.

To explore the CO desorption step, after the pretreatment in air, the IR cell was purged in He at 200°C for 1 h. Then 0.3% CO in He was introduced and a series of spectra were collected until the net absorbance was constant. At this moment, the CO was discontinued, leaving a flow of pure He. Figure 13 presents the spectra of adsorbed CO at different times as CO desorbs from the surface at constant temperature for the Cl-free and Cl-containing Pt/SiO_2 catalysts. The spectra show a small shift of the main IR band to lower wavenumbers as CO desorbs from the surface. This shift has been explained by a dipole–dipole interaction between the adsorbed CO molecules at high CO coverage (33–35). The time elapsed until similar IR intensities are detected is almost twice as long in the case of the Cl-containing catalyst compared to the Cl-free catalyst. Assuming that the CO desorption rate is first order with respect to CO surface concentration, rate constants of CO desorption were calculated for both catalysts using the expression $\ln(IA/IA_O) = -k_{CO\ des}t$, where IA is the integrated absorbance of the CO linear band and t the time in minutes. Figure 14 shows that within experimental error, the rate constant for CO desorption is the same ($k_{CO\ desorp} = 0.00493\ min^{-1} \pm 5\%$) for the Cl-free and the Cl-containing catalysts. Thus, the presence of Cl does not affect the rate of CO desorption. Furthermore, the wavenumber of the CO linear band at maximum coverage (Fig. 13) is similar for both catalysts, indicating that the active site for adsorption is the same in both cases. These findings support the conclusion that the poisoning effect of Cl is that it blocks the active sites for adsorption and reaction.

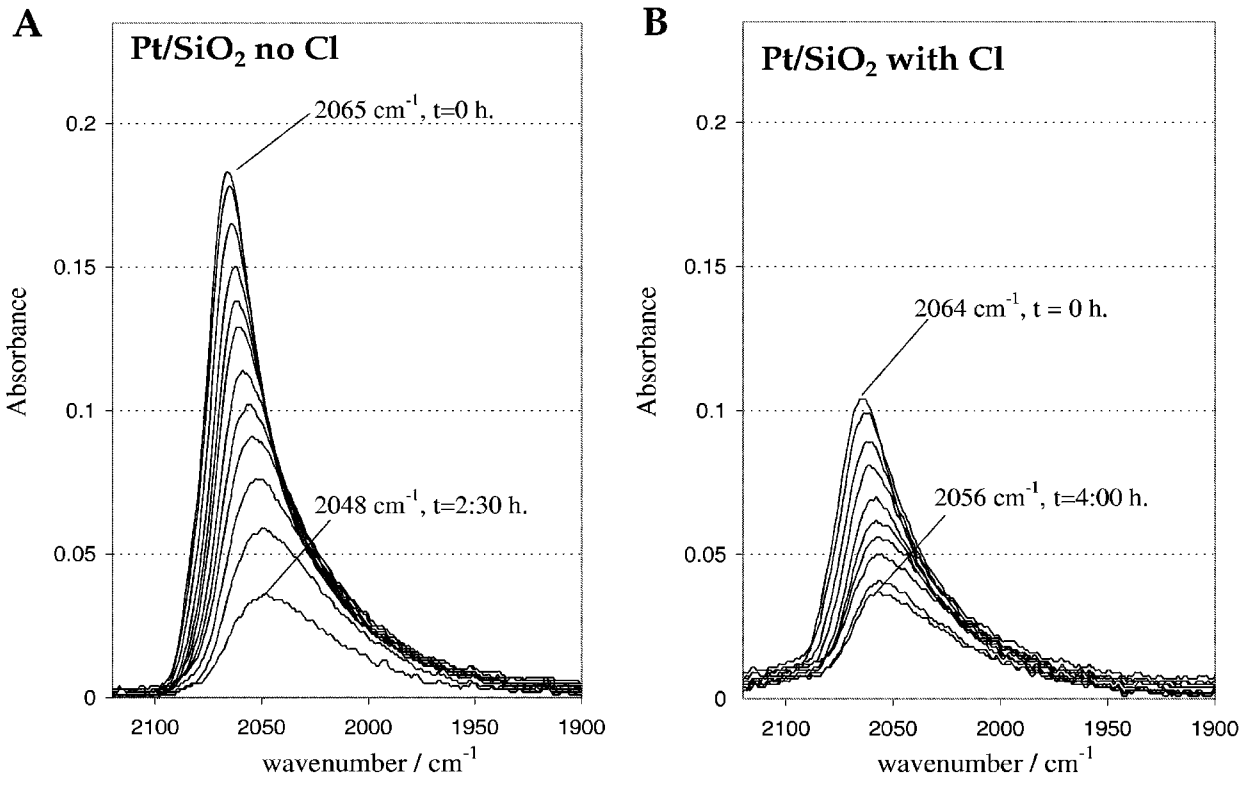

FIG. 13. FTIR spectra during CO desorption on Pt/silica at 200°C. (A) 2% Pt/silica no Cl. (B) 2% Pt/silica with Cl. Total flow rate, 120 cm^3/min pure He.

4. DISCUSSION

The above results provide a general qualitative understanding of the poisoning effect of Cl during oxidation reactions on Pt-supported catalysts. Several studies have shown the inferior performance of Pd and Pt catalysts prepared from Cl-containing precursors for methane oxidation (3–6, 8, 10, 12). Similar behavior has been reported for the combustion of higher hydrocarbons (13, 36) and during complete oxidation of toluene (11), as well as for propane oxidation (14). Our results for CO, methane, and ethane oxidation are consistent with the poisoning effect of chlorine previously reported in the literature. As it has been shown, this effect occurs not only when the precursor is the source of chlorine but also when Cl is added from an external source, such as HCl. This is a clear indication that Cl is mobile under the reaction conditions and leads to deactivation by blocking the active sites on the Pt surface.

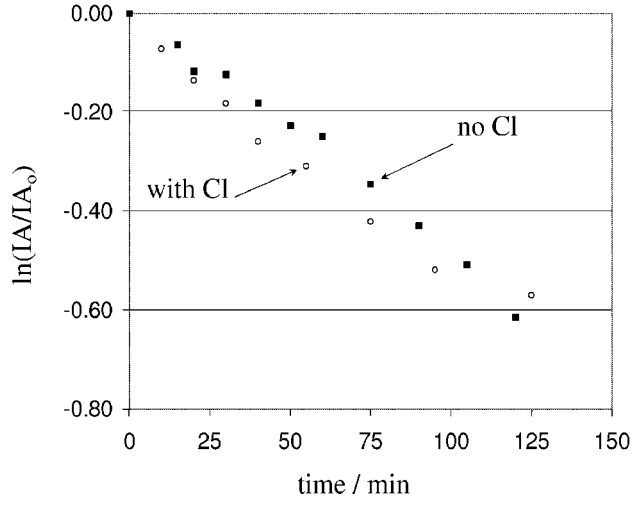

FIG. 14. Integrated Absorbance of CO linear band vs time during CO desorption on Pt/silica at 200°C. (■) 2% Pt/silica no Cl. (○) 2% Pt/silica with Cl.

Even though Cl is a strong inhibitor of the oxidation activity, it is a reversible poison, and the extent of Cl coverage depends on the pretreatment and support used. For example, after a 10-h reduction the HCl-impregnated Pt/SiO_2 catalyst recovered most of its initial activity, in agreement with results showing an activation of Pt/Al_2O_3 catalysts with time on stream reported by several authors (4, 20). Nonetheless, the removal of chlorine strongly depends on the reaction environment and temperature of the treatment as well as on the catalyst's support (9). Most studies reporting elimination of Cl from Pt/Al_2O_3 catalysts indicate that water plays a role in the activation treatments, either when it is a product of the oxidation reaction (5) or after addition as steam under a reducing atmosphere (37).

The kinetic results of the Cl-free catalyst impregnated with HCl indicate that at first chlorine is adsorbed mainly on the Al_2O_3 support (5, 13, 17), and during calcination a portion of the Cl migrates from the support and is readsorbed onto the Pt surface. The transport and mobility of chlorine on the catalyst's surface is also confirmed by the EXAFS and IR results. IR results indicate that no detectable CO adsorption on Pt occurs at low temperatures (60–100°C) on the Cl-containing catalyst, but as the catalyst temperature increases in the presence of oxygen and CO, the CO coverage increases. EXAFS data clearly show that there are no Pt–Cl bonds after reduction, but later, in the presence of oxygen, an oxychloroplatinum phase reappears surrounding a small core of reduced Pt atoms. Lieske *et al.* (15) was one of the first groups proposing the formation of oxychloroplatinum species under oxidizing conditions, $[Pt^{IV}(OH)_xCl_y]$ and $[Pt^{IV}O_xCl_y]$, to explain the redispersion of Pt at high temperatures, 500–600°C. These authors found that the formation of these species requires the presence of oxygen. The interaction between platinum, oxygen, and chlorine starts at temperatures below 300°C, promoting the formation of oxychloroplatinum species. Similar species have been reported in EXAFS analysis of the preparation (38) and redispersion (39, 40) of Pt/alumina (Cl) naphtha-reforming catalysts.

Thus, the kinetic and EXAFS results can only be explained if the Cl coming from HCl or evolved during reduction is reabsorbed on the support and subsequently released and readsorbed on the Pt surface during calcination. During reduction H_2 adsorbs dissociatively on the Pt surface and reacts with the adsorbed complex to likely yield HCl, which desorbs as a gas and is transported onto the support. Recent results on chlorinated Pt catalysts supported on model flat alumina substrates (41) indicate that no Cl is observed after reduction at 300°C. Therefore, the surface–Cl interaction during reduction is affected by the porous structure of the supported catalysts. In the case of HCl, this process can be pictured as follows (13, 42):

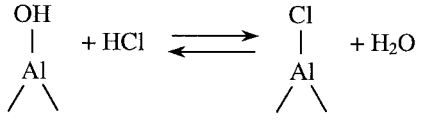

Depending on the time, temperature, and Cl-support interaction, Cl can be eliminated or remain adsorbed on the support. In the later case, calcination or oxidation pretreatments lead to desorption of Cl from the support and to the formation of a stable platinum oxychloride species (43, 44). Regardless of the detailed mechanism of Cl transport from the support to the metal and vice versa, i.e., surface diffusion vs gas-phase transport, all of the results show this dynamic interaction between Cl, Pt, and the support resulting in a specific catalytic activity.

Activity and FTIR results indicate that the ignition process changed in the presence of Cl. It has been reported that the reduction of the $Pt–O_x$ species occurs at lower temperatures than those for chlorinated species in Pt- and Pd-supported catalysts (44). This could explain why CO can adsorb on the Cl-free catalyst at low temperatures whereas, in the Cl-containing catalyst, heating to much higher temperature is required to observe CO adsorption, and later reaction, on reduced Pt surface after partial reduction of $PtCl_xO_y$ species (Fig. 12). The difference in the light-off temperature can, therefore, be explained by the different reducibility of PtO_x and $PtCl_xO_y$ species.

Likewise, the different apparent activation energies for CO oxidation observed in Fig. 1A can be attributed to a temperature-dependent variation of the number of active sites in the Cl-containing catalyst. The IR spectra of CO adsorbed during reaction clearly indicate that the amount of linearly adsorbed CO on Pt for the Cl-containing catalysts increases with temperature, whereas for the Cl-free catalyst no change is observed with increasing temperature (Fig. 12). The percentage of available sites for CO adsorption in the catalyst with Cl was estimated as the ratio of the integrated absorbances of the CO linear band in the Cl-containing catalyst and in the Cl-free catalyst at the same temperature. These results are presented in Table 2. The assumption in the previous calculations is that CO adsorbs in all the available sites, which is the case at the low temperatures ($T < 140$°C) used to obtain the activation energies. With these data the reaction rates of CO oxidation in Pt/Al_2O_3 with Cl were recalculated and included in the Arrhenius plot in Fig. 1A. The new value of the activation energy, 63.9 kJ/mol, is very similar to that obtained for the Cl-free catalyst, 59.9 kJ/mol. Therefore, changes in the activation energy for CO oxidation can be explained by the increase in the number of available active sites in the Pt/alumina with Cl as the temperature increases. This result implies that chlorine is mobile on the catalytic surface under reaction conditions and confirms that the primary mechanism of Cl poisoning is due to site blocking of the reduced Pt surface.

4.1. Model of Cl Poisoning

The EXAFS and activity results, presented under the different reaction conditions, clearly show the dynamic role of the support, which can store Cl during reduction only

TABLE 2

Fraction of Available Active Sites at Different Temperatures for Cl-Containing Catalyst

T (°C)	% Available sites	% Blocked sites
60	7.6	92.4
80	14.2	85.8
100	18.2	81.8
120	26.1	73.9
140	39.2	60.8
160	45.9	54.1

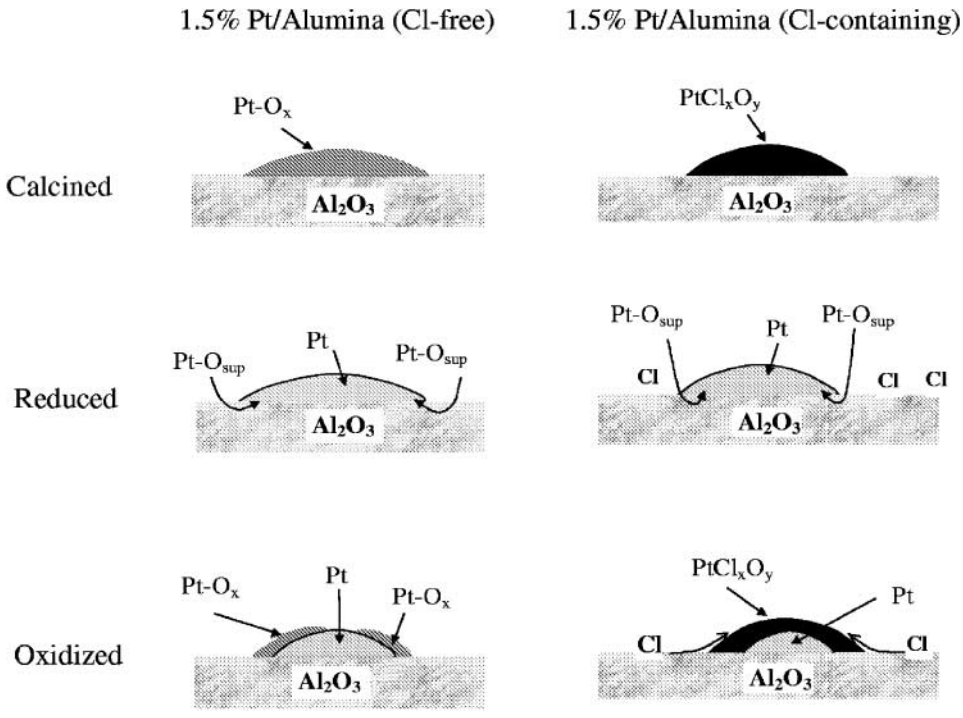

FIG. 15. Model depicting the Pt species after the various treatments.

to release it during oxidation pretreatment or reaction to be readsorbed on the Pt surface and poison its activity. Based on the catalyst activities and characterization results, we propose the model shown in Fig. 15, depicting the Pt species after the various treatments. Upon calcination, the Pt is present as a platinum(IV) oxide phase (Cl free) or a platinum(IV) oxychloride phase (with Cl). Since there are no apparent Pt–Pt bonds, the oxide is present as adsorbed molecular species or very small, highly disordered particles. Reduction of the calcined catalysts leads to small metallic particles in contact with the oxygen ions from the alumina support. In the Cl-containing catalyst, there are no Pt–Cl bonds, as the chlorine has been transported onto the support during reduction. Treatment in oxygen at 300°C oxidized the Pt surface on both catalysts. In the case of the Cl-containing catalyst, the transport of chlorine back from the support onto the Pt surface leads to the formation of an oxychloroplatinum phase with little exposed low-valent Pt. Nonetheless, in both cases, with and without Cl, the Pt particles are not fully oxidized, and there remains a small core of reduced metal. In the Cl-free catalyst low-valent or metallic Pt atoms are exposed to the reactants.

Determining the nature of the active surface during reaction is not straightforward. It has been suggested that on large Pt particles there is only a layer of chemisorbed oxygen, while on smaller highly dispersed platinum particles there is a layer of platinum oxide during methane (28) and toluene oxidation (45). Our activity results with Pt/Al_2O_3 catalysts after different pretreatments (Fig. 6) confirm that fully oxidized Pt particles exhibit low activity compared to that on a partially oxidized, metallic surface. The EXAFS and IR spectra indicate that both oxidized and low-valent Pt are present under oxidation reaction conditions. This model agrees well with previous ones (20, 21, 28), which concluded that neither a fully reduced nor a fully oxidized surface is optimal for methane oxidation. In addition, the catalytic activity correlates with the amount of exposed metallic Pt. The highest activity, for example for CO oxidation, was on the reduced catalyst without Cl. Oxidation at 350°C in 100% O_2 lowered the activity. The calcined catalyst, which contained no metallic Pt, had still lower activity. Similar conclusions can be made for the Pt/alumina with Cl. The IR indicates that there is no detectable CO adsorption at low temperatures (60–100°C) and the activity is low. Although there are likely surface Pt–O bonds, there is little activity. As the reaction temperature increases, however, the CO coverage increases. Since the IR frequency is similar to that in the Cl-free catalyst, it is likely that the CO is adsorbed on exposed metallic sites generated by surface reduction at higher temperature.

5. CONCLUSIONS

Alumina and silica supports have been used to prepare different Pt catalysts with and without Cl. Independent of the precursor, the presence of Cl significantly decreases the activity of Pt-supported catalysts for CO, methane, and ethane oxidation. This poisoning effect depends on the Cl coverage, which in turn depends on the pretreatment, the reaction conditions, and the support–Cl interaction.

Both Cl-free and Cl-containing catalysts present higher activity after reduction in H_2 compared to that of the catalysts that have only undergone calcination. The activity of Cl-free catalysts after addition of HCl and pretreatment in air is similar to that of the Cl-containing catalyst.

A model is proposed to describe the different Pt species present after different pretreatments. This model indicates that transport of Cl from the metal surface to the support occurring under reducing conditions is reversed when oxygen is present in the gas phase. While pretreatments in air at temperatures at about 300°C affect this migration, prolonged time on stream (reaction conditions) or higher temperature pretreatments can eliminate Cl from the Pt surface and support. The model proposes that the reduced and partially oxidized Pt particles are the main active phases during the oxidation reaction on Pt-supported catalysts at conditions similar to those used in this work. Obviously, the state of the surface and the kinetics of the Cl–metal and Cl–support interaction will change if the reaction environment is different.

Kinetic studies complemented with EXAFS and IR results show that the main effect of Cl is to block the metal surface, decreasing the number of active sites. The extent of the blockage depends on the temperature and reaction conditions used as well as on the capacity of the support to adsorb Cl.

ACKNOWLEDGMENTS

Use of the Advanced Photon Source was supported by the U.S. Department of Energy, Office of Basic Energy Sciences, Office of Science (DOE-BES-SC), under Contract W-31-109-Eng-38. The MR-CAT is funded by the member institutions and DOE-BES-SC under contracts DE-FG02-94ER45525 and DE-FG02-96ER45589. We also acknowledge partial funding of this work from a NSF GOALI 99-04033 grant.

REFERENCES

1. Zwinkels, M. F. M., Jaras, S. G., Menon, P. G., and Griffin, T. A., *Catal. Rev.–Sci. Eng.* **35**, 319 (1993).
2. Gupta, A. K., and Lilley, D. G., *J. Prop. Pow.* **10**(2), 137 (1994).
3. Simone, D. O., Kennelly, T., Brungard, N. L., and Farrauto, R. J., *Appl. Catal.* **70**, 87 (1991).
4. Marceau, E., Che, M., Saint-Just, J., and Tatibouet, J. M., *Catal. Today* **29**, 415 (1996).
5. Marceau, E., Lauron-Pernot, H., and Che, M., *J. Catal.* **197**, 394 (2001).
6. Roth, D., Gelin, P., Primet, M., and Tena, E., *Appl. Catal. A* **203**, 37 (2000).
7. Malet, P., Munuera, G., and Caballero, A., *J. Catal.* **115**, 567 (1989).
8. Pecchi, G., Reyes, P., Gómez, R., López, T., and Fierro, J. L. G., *Appl. Catal. B* **17**, L7 (1998).
9. Reyes, P., Oportus, M., Pecchi, G., Fréty, R., and Moraweck, B., *Catal. Lett.* **37**, 193 (1996).
10. (a) Baldwin, T. R., and Burch, R., *Appl. Catal.* **66**, 337 (1990). (b) Baldwin, T. R., and Burch, R., *Catal. Lett.* **6**, 131 (1990).
11. Paulis, M., Peyrard, H., and Montes, M., *J. Catal.* **199**, 30 (2001).
12. Peri, S. S., and Lund, C. R., *J. Catal.* **152**, 410 (1995).
13. Cant, N. W., Angove, D. E., and Patterson, M. J., *Catal. Today* **44**, 93 (1998).
14. Marecot, P., Fakche, A., Kellali, B., Mabilon, G., Prigent, M., and Barbier, J., *Appl. Catal. B* **3**, 283 (1994).
15. Lieske, H., Lietz, G., Spindler, H., and Volter, J., *J. Catal.* **81**, 8 (1983).
16. Hwang, C. P., and Yeh, C. T., *J. Mol. Catal. A* **112**, 295 (1996).
17. Lebedeva, O. E., Chiou, W., and Sachtler, W., *Catal. Lett.* **66**, 189 (2000).
18. Mordente, M., and Rochester, C., *J. Chem. Soc. Faraday Trans. 1* **85**(10), 3495 (1989).
19. Zhou, Y., Wood, M. C., and Winograd, N., *J. Catal.* **146**, 82 (1994).
20. (a) Burch, R., and Loader, P. K., *Appl. Catal. B* **5**, 149 (1994). (b) Burch, R., and Loader, P. K., *Appl. Catal. A* **122**, 169 (1995).
21. Yang, S., Maroto-Valiente, A., Benito-Gonzalez, M., Rodriguez-Ramos, I., and Guerrero-Ruiz, A., *Appl. Catal. B* **28**, 223 (2000).
22. Segre, C. U., Leyarovska, N. E., Lavender, W. M., Plag, P. W., King, A. S., Kropf, A. J., Bunker, B. A., Kemmer, K. M., Dutta, P., Duran, R. S., and Kaduk, J., *in* "CP521, Synchroton Radiation Instrumentation: 11th U.S. National Conference" (P. Pianetta, *et al.*, Eds.), p. 419. American Institute of Physics, New York, 2000.
23. Yazawa, Y., Kagi, N., Komai, S., Satsuma, A., Marakami, Y., and Hattori, T., *Catal. Lett.* **72** (3–4), 157 (2001).
24. Ressler, T. J., *J. Sync. Rad.* **5**, 118 (1998).
25. Lytle, F. W., Sayers, D. E., and Stern, E. A., *Physica B* **158**, 701 (1989).
26. Vaarkamp, M., Modica, F. S., Miller, J. T., and Koningsberger, D. C., *J. Catal.* **144**, 611 (1993).
27. Bazin, D., Triconnet, A., and Moureaux, P., *Nucl. Instrum. Methods Phys. Res. Sect. B* **97** (1–4), 41 (1995).
28. Jackson, S. D., Glanville, B. M., Willis, J., Mclellan, G. D., Webb, G., Moyes, R. B., Simpson, S., Wells, P. B., and Whyman, R., *J. Catal.* **139**, 207 (1993).
29. (a) Hicks, R., Qi, H., Young, M. L., and Lee, R. G., *J. Catal.* **122**, 280 (1990). (b) Hicks, R., Qi, H., Young, M. L., and Lee, R. G., *J. Catal.* **122**, 295 (1990).
30. Bernal, S., Blanco, G., Gatica, J. M., Larese, C., and Vidal, H., *J. Catal.* **200**, 411 (2001).
31. Dulaurent, O., and Bianchi, D., *Appl. Catal. A* **196**, 271 (2000).
32. Hertz, R. K., and Shinouskis, E. J., *Appl. Surf. Sci.* **19**, 373 (1984).
33. Araya, P., Porod, W., and Wolf, E. E., *Surf. Sci.* **230**, 245 (1990).
34. (a) Crossley, A., and King, D. A., *Surf. Sci.* **68**, 528 (1977). (b) Crossley, A., and King, D. A., *Surf. Sci.* **95**, 131 (1980).
35. Lyons, K. J., Xie, J., Mitchell, W. J., and Weinberg, W. H., *Surf. Sci* **325** (1–2), 85 (1995).
36. Garetto, T. F., and Apesteguía, C. R., *Catal. Today* **62**, 189 (2000).
37. Straguzzi, G. I., Aduriz, H. R., and Gigola, C. E., *J. Catal.* **66**, 171 (1980).
38. Lagarde, P., Murata, T., Vlaic, G., Freund, E., Dexpert, H., and Bournonville, J. P., *J. Catal.* **84**, 333 (1983).
39. Le Normand, F., Borgna, A., Garetto, T. F., Apesteguia, C. R., and Moraweck, B., *J. Phys. Chem.* **100**, 9068 (1996).
40. Borgna, A., Garetto, T. F., Apesteguia, C. R., Le Normand, F., and Moraweck, B., *J. Catal.* **186**, 433 (1999).
41. Borg, H. J., van den Oetelaar, L. C. A., and Niemantsverdriet, J. W., *Catal. Lett.* **17**, 81 (1993).
42. Castro, A. A., Scelza, O. A., Benvenuto, E. R., Baronetti, G. T., and Parera, J. M., *J. Catal.* **69**, 222 (1981).
43. Barbier, J., Bahloul, D., and Marecot, P., *Catal. Lett.* **8**, 327 (1991).
44. Contescu, C., Macovei, D., Craiu, C., Teodorescu, C., and Schwarz, J. A., *Langmuir* **11**, 2031 (1995).
45. Grbić, B., Radić, N., and Terlecki-Baričević, A., *Sci. Sin.* **30**(3), 179 (1998).